



Attenuation of the Hepatoprotective Effects of Ileal Apical Sodium Dependent Bile Acid Transporter (ASBT) Inhibition in Choline-Deficient L-Amino Acid-Defined (CDAA) Diet-Fed Mice

Anuradha Rao¹, Ivo P. van de Peppel², Sanjeev Gumber³, Saul J. Karpen¹ and Paul A. Dawson^{1*}

¹ Department of Pediatrics, Emory University School of Medicine, Atlanta, GA, United States, ² Section of Molecular Metabolism and Nutrition, Department of Pediatrics, University Medical Center Groningen, University of Groningen, Groningen, Netherlands, ³ Division of Pathology, Yerkes National Primate Research Center, Emory University, Atlanta, GA, United States

OPEN ACCESS

Edited by:

Shannon Glaser,
Texas A&M Health Science Center,
College of Medicine, United States

Reviewed by:

Jose A. Uranga,
Rey Juan Carlos University, Spain
Yuji Naito,
Kyoto Prefectural University of
Medicine, Japan

*Correspondence:

Paul A. Dawson
paul.dawson@emory.edu

Specialty section:

This article was submitted to
Gastroenterology,
a section of the journal
Frontiers in Medicine

Received: 08 November 2019

Accepted: 10 February 2020

Published: 25 February 2020

Citation:

Rao A, Peppel IPvd, Gumber S,
Karpen SJ and Dawson PA (2020)
Attenuation of the Hepatoprotective
Effects of Ileal Apical Sodium
Dependent Bile Acid Transporter
(ASBT) Inhibition in Choline-Deficient
L-Amino Acid-Defined (CDAA)
Diet-Fed Mice. *Front. Med.* 7:60.
doi: 10.3389/fmed.2020.00060

Non-alcoholic fatty liver disease (NAFLD) is a major growing worldwide health problem. We previously reported that interruption of the enterohepatic circulation of bile acids using a non-absorbable apical sodium-dependent bile acid transporter inhibitor (ASBTi; SC-435) reduced the development of NAFLD in high fat diet fed mice. However, the ability of ASBTi treatment to impact the progression of NAFLD to non-alcoholic steatohepatitis (NASH) and fibrosis in a diet-induced mouse model remains untested. In the current study, we assessed whether ASBTi treatment is hepatoprotective in the choline-deficient, L-amino acid-defined (CDAA) diet model of NASH-induced fibrosis.

Methods: Male C57Bl/6 mice were fed with: (A) choline-sufficient L-amino acid-defined diet (CSAA) (31 kcal% fat), (B) CSAA diet plus ASBTi (SC-435; 60 ppm), (C) CDAA diet, or (D) CDAA diet plus ASBTi. Body weight and food intake were monitored. After 22 weeks on diet, liver histology, cholesterol and triglyceride levels, and gene expression were measured. Fecal bile acid and fat excretion were measured, and intestinal fat absorption was determined using the sucrose polybehenate method.

Results: ASBTi treatment reduced bodyweight gain in mice fed either the CSAA or CDAA diet, and prevented the increase in liver to body weight ratio observed in CDAA-fed mice. ASBTi significantly reduced hepatic total cholesterol levels in both CSAA and CDAA-fed mice. ASBTi-associated significant reductions in hepatic triglyceride levels and histological scoring for NAFLD activity were observed in CSAA but not CDAA-fed mice. These changes correlated with measurements of intestinal fat absorption, which was significantly reduced in ASBTi-treated mice fed the CSAA (85 vs. 94%, $P < 0.001$) but not CDAA diet (93 vs. 93%). As scored by Ishak staging of Sirius red stained liver sections, no hepatic fibrosis was evident in the CSAA diet mice. The CDAA diet-fed mice developed hepatic fibrosis, which was increased by the ASBTi.

Conclusions: ASBT inhibition reduced intestinal fat absorption, bodyweight gain and hepatic steatosis in CSAA diet-fed mice. The effects of the ASBTi on steatosis and fat absorption were attenuated in the context of dietary choline-deficiency. Inhibition of intestinal absorption of fatty acids may be involved in the therapeutic effects of ASBTi treatment.

Keywords: liver, triglyceride, fibrosis, fat absorption, cholesterol

INTRODUCTION

Parallel to the global rise in obesity, the disease burden related to non-alcoholic fatty liver disease (NAFLD) is emerging as a major worldwide problem. The number of adults and children with NAFLD is steadily increasing and the current global prevalence is estimated at 24% (1, 2). NAFLD comprises a spectrum of disease states, from non-symptomatic hepatic steatosis to non-alcoholic steatohepatitis (NASH) and liver fibrosis. NAFLD also increases the morbidity and mortality associated with type 2 diabetes mellitus, cardiovascular disease, and chronic kidney disease (3). Unfortunately, an incomplete understanding and lack of experimental NAFLD/NASH animal models that faithfully reproduce the human pathophysiology has slowed the development of new therapies (4). Recently, bile acid-related pathways have emerged as an important therapeutic target for disorders of glucose and lipid metabolism (5). Under physiological conditions, bile acid synthesis and enterohepatic cycling are tightly regulated to maintain a relatively constant whole-body bile acid pool size and restrict the systemic distribution of bile acids. After their secretion along with bile into the duodenum, about 95% of the bile acids are reabsorbed by the apical sodium-dependent bile acid transporter (ASBT; also called the ileal bile acid transporter, IBAT) in the distal small intestine, thereby limiting their flux into the colon. This system is tightly controlled in part by bile acid signaling via the farnesoid-X receptor (FXR) in the liver and intestine. The intestinal microbiota harbor enzymes to deconjugate and convert primary bile acids into secondary bile acids, changing the bile acid pool size, composition, and physicochemical properties (6). These changes alter signaling through FXR and other bile acid-activated receptors, and modulates the metabolic response to bile acids (7).

Several bile acid-based approaches are currently under investigation as potential therapies for liver diseases, including NAFLD. Obeticholic acid, a derivative of the naturally occurring FXR agonist chenodeoxycholic acid (CDCA), improved liver biochemistry and histology scores in NASH patients (8, 9).

Abbreviations: ASBT, Apical sodium-dependent bile acid transporter; ASBTi, Apical sodium-dependent bile acid transporter inhibitor; BW, bodyweight; CA, cholic acid; CDAA, choline-deficient, L-amino acid-defined; CSAA, choline-sufficient L-amino acid-defined; DCA, deoxycholic acid; FXR, farnesoid-X receptor; GC, gas chromatography; HCA, hyodeoxycholic acid; IBAT, ileal bile acid transporter; LCA, lithocholic acid; MCA, muricholic acid; MCD, methionine/choline-deficient; NAFLD, non-alcoholic fatty liver disease; NAS, NAFLD Activity Score; NASH, non-alcoholic steatohepatitis; PC, phosphatidylcholine; VLDL, very low density lipoprotein.

In addition, we have shown that interruption of the bile acid enterohepatic circulation by an ASBT inhibitor (ASBTi), SC-435, prevented hepatic lipid accumulation and improved markers of NAFLD in mice fed a high fat diet (10). Although these results and similar findings in high fat diet-fed *Ldlr*^{-/-} Leiden mice demonstrated a robust effect of ASBT inhibition on hepatic lipid accumulation, the effects of ASBT inhibition on the progression from hepatic steatosis to steatohepatitis and fibrosis remain unclear (10, 11). Feeding a Western-type diet (high fat, sucrose, and cholesterol) to mice typically models aspects of the human condition including successfully inducing hepatic lipid accumulation. However, progression from steatosis to NASH and fibrosis is generally limited and highly variable (12–14). Therefore, other dietary, genetic or toxic interventions, or combinations thereof, are required to induce development of NASH in animal models. One widely used intervention for dietary induction of NASH and subsequent fibrosis is the methionine/choline-deficient (MCD) diet. Depriving mice of dietary choline impairs hepatic secretion of very low density lipoproteins (VLDL) and results in hepatic steatosis, oxidative stress, cell death, and increases in cytokine levels (15). Combined with methionine deficiency, the mice develop extensive inflammation after 2 weeks and significant fibrosis after 6 weeks (12). However, MCD diet-fed mice generally lose considerable bodyweight and show no insulin resistance (or even increased sensitivity), conditions that poorly correlate with development of NASH in humans (16, 17). In this current study we assessed the effects of ASBTi treatment on development of NAFLD and fibrosis using a choline-deficient L-amino acid-defined (CDAA) diet, which has been shown to successfully induce hepatic steatosis and subsequent fibrosis after 22 weeks without bodyweight loss (18, 19).

MATERIALS AND METHODS

Animals

Male C57Bl/6J mice aged 10 weeks were obtained from Jackson Laboratories. Animals were group-housed with 4 mice per ventilated cage (Super Mouse 750 Microisolator System; Lab Products) containing bedding (1/8" Bed-O-Cobbs; Andersons Lab Bedding Products) in the same temperature (22°C) and light/dark cycle (12-h; 7 AM to 7 PM) controlled room of the animal facility to minimize environmental differences. Mice were fed *ad libitum* for 22 weeks with either a choline-sufficient L-amino acid-defined control diet (CSAA, Catalog # 518754; Dyets Inc., Bethlehem, PA, USA) or choline-deficient L-amino acid-defined diet (CDAA, Catalog # 518753; Dyets Inc., Bethlehem,

PA, USA) with or without 0.006% (w/w) of the ASBTi (SC-435). This amount of ASBTi in the diet provides a dose of ~11 mg/kg/day of SC-435 (10). The CSAA and CDAA diets contain 31% of calories as fat (in the form of corn oil and partially hydrogenated vegetable oil; fatty acid composition: 23.4% saturated, 52.1% monounsaturated, 24.5% polyunsaturated) and have no added cholesterol. Food consumption was measured by weighing new and remaining food two times weekly. Calorie intake was calculated by multiplying the weight of the food consumed by their caloric density. During the final week on diet, the mice were individually housed to measure fat absorption and fecal bile acid and neutral sterol excretion.

Animal Experiments

During the final week of CSAA and CDAA (+/- ASBTi) diet feeding, mice received powdered diet containing 0.7% sucrose polybehenate (w/w) (20). Sucrose polybehenate is not absorbed in the intestine. Therefore, by comparing the ratio of behenic acid to total fatty acids in the diet and feces, the fractional fat absorption can be calculated without being reliant on food intake measurements. Powdered diet was placed in a feeding jar in the cage and replaced every 2–3 days. Feces were collected for individual mice during the final 3 days of the experiment and used for fatty acid, neutral sterol and bile acid measurements. After, mice were sacrificed and tissues collected for further analysis. Mice were anesthetized using isoflurane. Blood was obtained via cardiac puncture, centrifuged and the plasma was stored at -80°C . Livers were excised, weighed and pieces collected for subsequent histology analysis. Remaining liver tissue was snap frozen in liquid nitrogen. The small intestines were excised, measured, cut into five equal length segments, flushed with ice cold phosphate buffered solution (PBS) and snap frozen in liquid nitrogen. The length of the colon was measured, divided into proximal (60%) and distal (40%) segments, flushed with ice cold PBS and immediately snap frozen in liquid nitrogen.

Fatty Acid Measurements

Weighed samples of the synthetic diet and feces were saponified with methanolic NaOH, extracted with hexane, and converted to methyl esters. Samples were analyzed using gas chromatography (GC) to quantitate the fatty acid methyl esters and determine the amount of behenic acid (C22:0), saturated (14:0, 16:0, 18:0), monounsaturated (C18:1), and polyunsaturated (18:1, 18:2, 18:3 ω 3, 20:5 ω 3, 22:6 ω 3) fatty acids as previously described (21, 22). Each chromatogram was examined to verify the identification of constituent fatty acids and for quality control.

Histology

The livers were removed, weighed, and a portion was fixed in 10% neutral buffered formalin, embedded in paraffin, sectioned at 5 μm , and stained with hematoxylin and eosin. Sirius red staining was performed using the paraffin-embedded liver sections (method adapted from Picosirius Red Stain Kit, Polysciences, Inc., Warrington, PA, USA). The liver histology was assessed in a blinded fashion by a veterinary pathologist (S.G.) for steatosis, lobular inflammation, and hepatocellular ballooning to derive the NAFLD Activity Score (NAS) as described (23). Sirius red stained

sections were blindly assessed by S.G. for Ishak Stage using the scores adapted from Ishak et al. (24).

Hepatic and Jejunal Lipids

Hepatic lipids were extracted according to a protocol based on the Folch method (25). Briefly, lipids were extracted from ~60 mg of tissue using 3 ml of chloroform:methanol (2:1) and incubated at 55°C for at least 2 h. Phases were split by adding 0.05% (v/v) sulfuric acid in water and centrifugation at 1,500 rpm for 15 min. Part of the bottom layer was transferred, dried under nitrogen and dissolved in 2% (v/v) Triton X-100 in water. Hepatic concentrations of total cholesterol (Pointe Scientific, C7510-01-906), free cholesterol (Fujifilm Wako Diagnostics, Cat# 993-02501), and triglyceride (Fujifilm Wako Diagnostics, Cat# 994-02891 and Cat# 990-02991) were subsequently measured by enzymatic assays.

Gene Expression

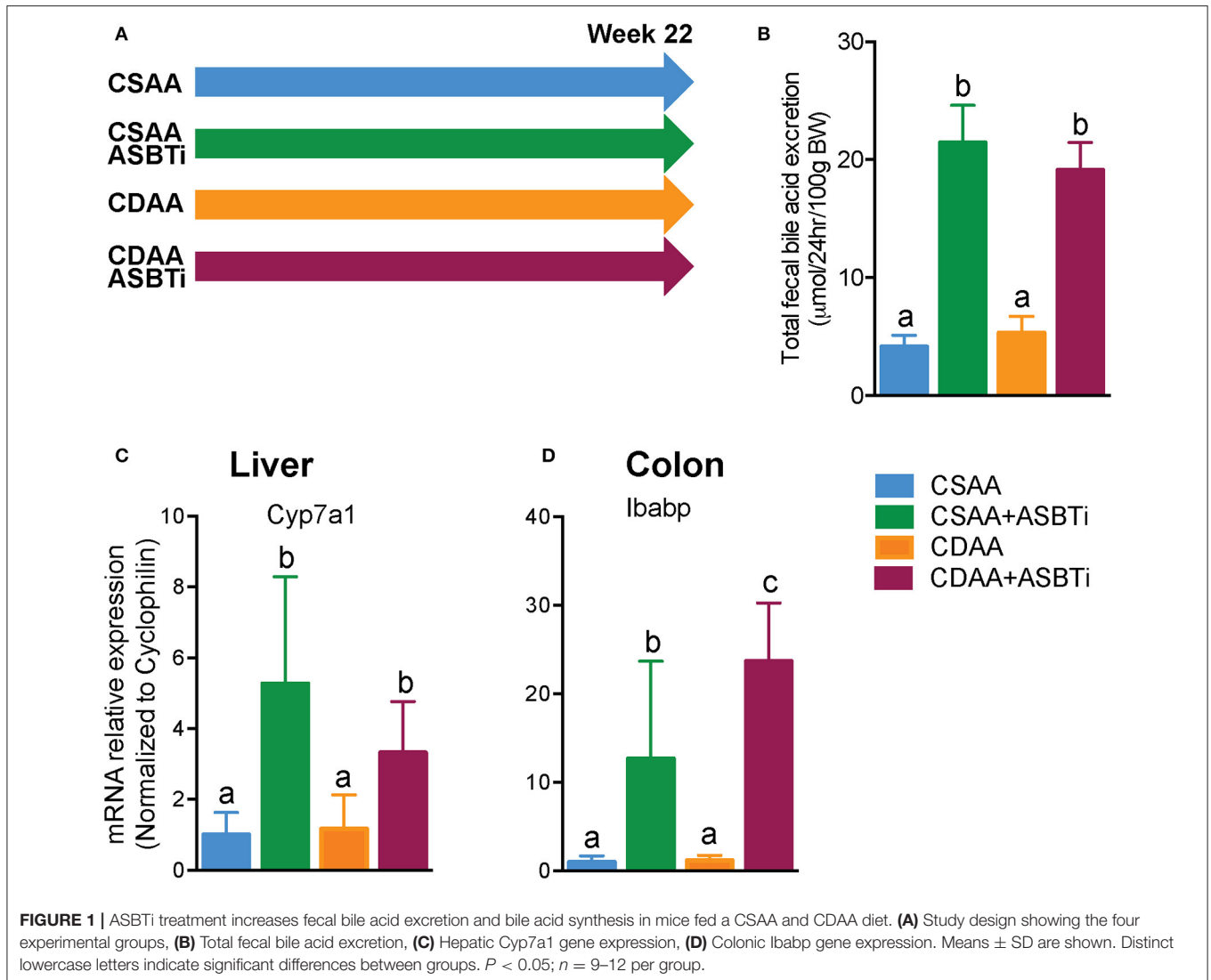
Total RNA was isolated from proximal colon and liver using a miRNeasy kit (Qiagen, Cat# 74106). Reverse transcriptase polymerase chain reaction (RT-PCR) was performed with 1 μg RNA using a high capacity cDNA reverse transcription kit (Applied Biosystems, Cat# 4368814). Real-time quantitative PCR was performed with a Sybr Green master mix (Applied Biosystems, Cat# 4309155) using a StepOne Plus real time PCR system (Applied Biosystems). The mRNA expression levels were calculated based on the $\Delta\Delta\text{-CT}$ method; values are means of triplicate determinations and expression was normalized using cyclophilin. The sequences of the primers used has been published previously (26).

Fecal Bile Acids and Neutral Sterols

Fecal pellets were sorted, air-dried, weighed and mechanically homogenized. Neutral sterols and bile acids were extracted from 50 mg of feces or diet as described (27). Briefly, samples were heated for 2 h at 80°C with a mixture of 1 M sodium hydroxide and methanol (3:1). Neutral sterols were then extracted twice with 2 ml petroleum ether and derivatized with *N*, *O*-Bis(trimethylsilyl)trifluoroacetamide (BSTFA)-pyridine-trimethylchlorosilane (TMCS) (5:5:0.1). Bile acids were quantitatively extracted from feces, isolated on Sep-Pak C-18 columns, methylated with methanol/acetyl chloride (20:1) and derivatized with BSTFA-pyridine-TMCS (5:5:0.1) (27). Both neutral sterols and bile acids were measured by gas chromatography (GC) (28). The total amount of bile acids or neutral sterols was calculated as the sum of the individual species.

Statistical Analyses

Data are presented as means \pm standard deviation (SD), unless stated otherwise. Statistical analyses were performed and graphs were created using GraphPad Prism 8 (GraphPad Software, La Jolla, CA, USA). Differences between groups were assessed by one-way ANOVA with Tukey's *post-hoc* test except for Ishak Stage, which was tested using a Chi-Squared test. Different lowercase letters indicate statistically significant differences ($P < 0.05$) between groups.



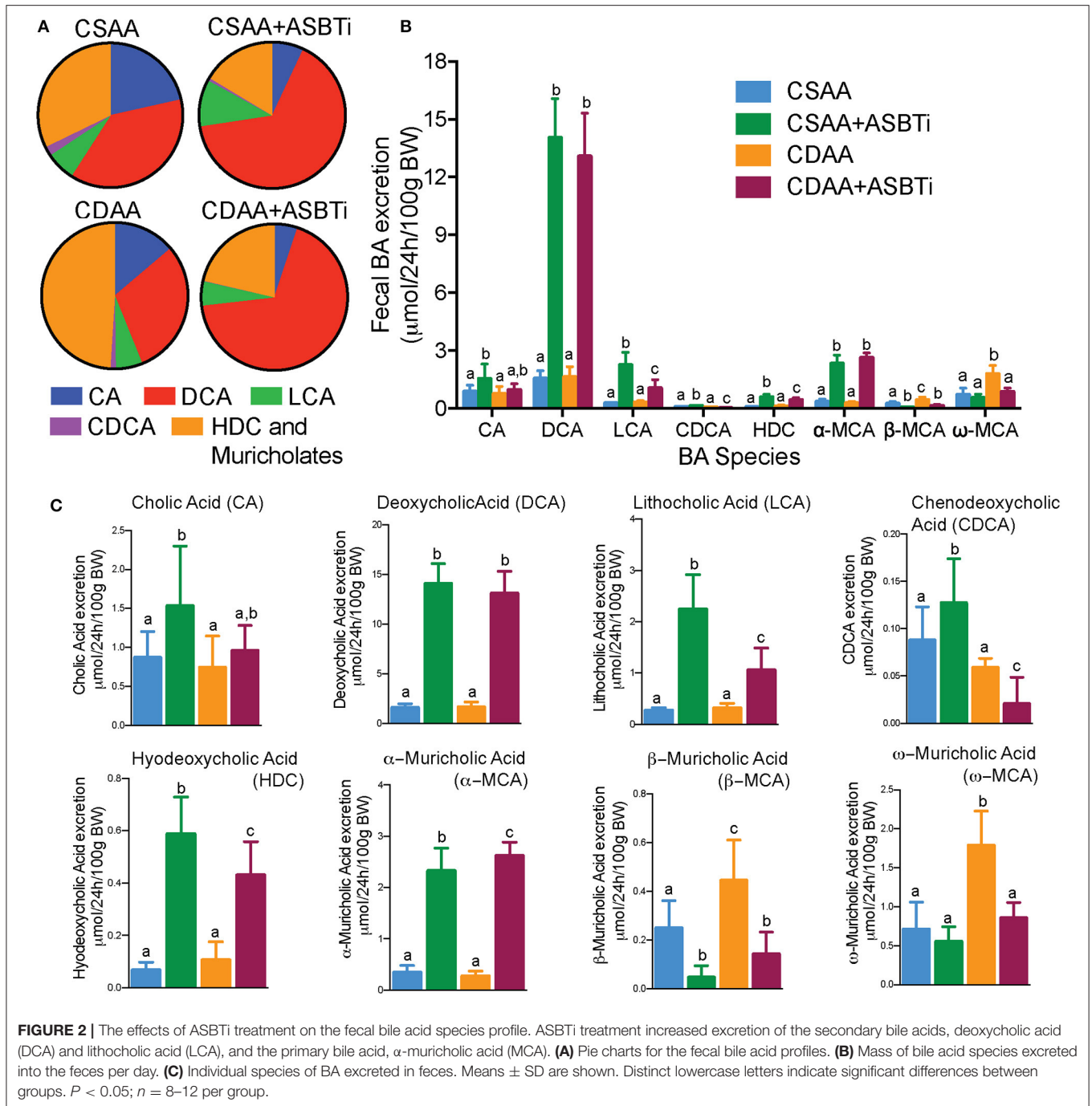
RESULTS

ASBT Inhibitor Treatment Reduces Bodyweight Gain in CSAA and CDAA Diet-Fed Mice

To determine whether ASBT inhibition can prevent development of NASH and fibrosis in mice, male C57Bl/6J mice were fed a choline-deficient L-amino-defined diet (CDAA) or a choline-sufficient control diet (CSAA) with or without an ASBTi for 22 weeks (**Figure 1A**). ASBTi treatment increased total fecal bile acid excretion by approximately 5-fold in CSAA (4.1 vs. 21.4 $\mu\text{mol}/24 \text{ h}/100 \text{ g BW}$, $P < 0.001$) and 4-fold in CDAA diet-fed mice (5.3 vs. 19.1 $\mu\text{mol}/24 \text{ h}/100 \text{ g BW}$, $P < 0.001$) (**Figure 1B**). Interruption of the enterohepatic circulation of bile acids was confirmed by gene expression measurements, with increases in hepatic cholesterol 7 α -hydroxylase (*Cyp7a1*) mRNA as a marker of bile acid synthesis, and colonic intestinal bile acid-binding protein (*Ibabp*) mRNA as a marker of colon bile acid

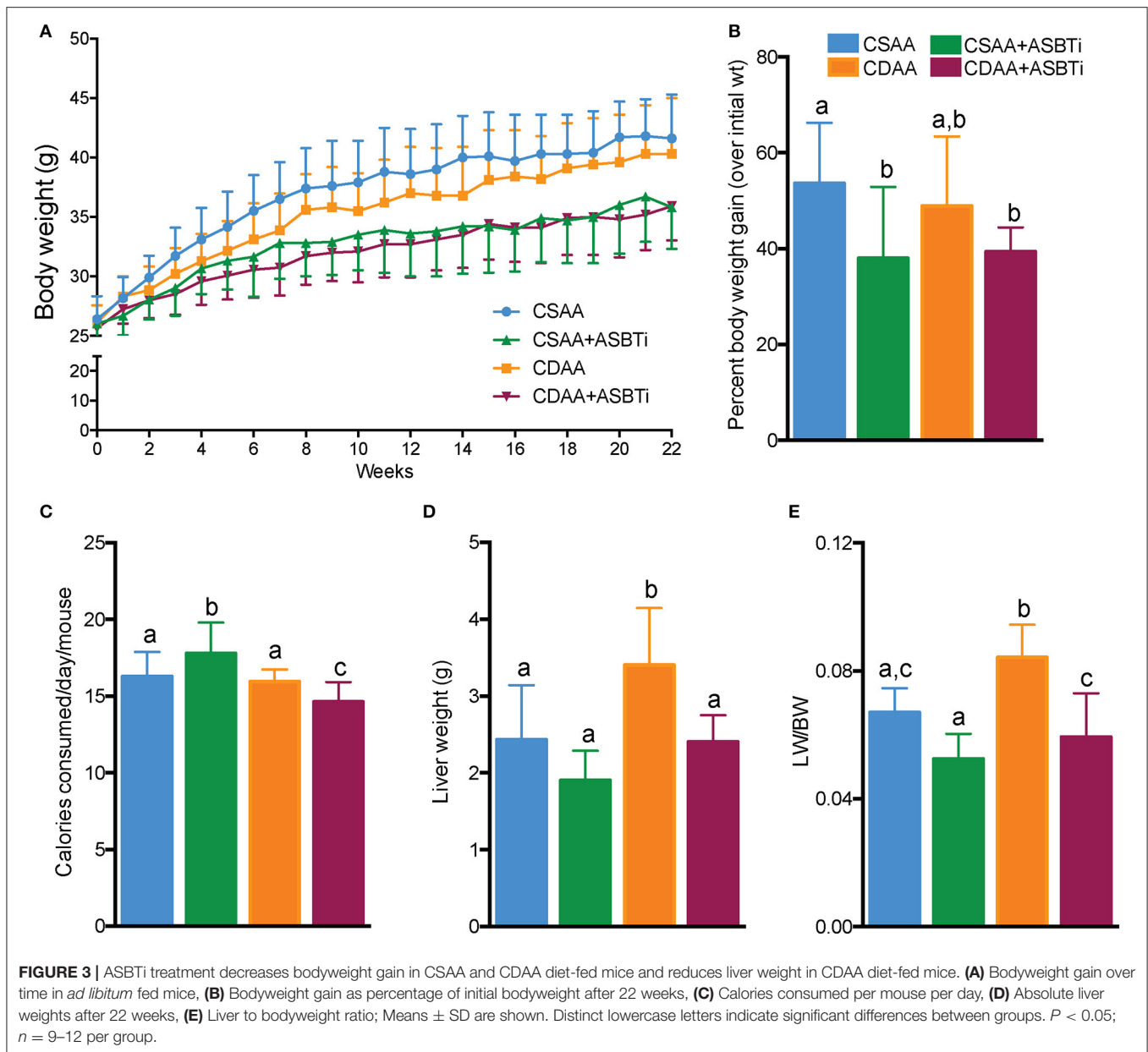
exposure (**Figures 1C,D**) in both the CSAA and CDAA diet-fed mice.

Inhibiting the ASBT in mice has been shown to increase the proportion of cholic acid (CA) plus its bacterial dehydroxylation product deoxycholic acid (DCA) and to reduce the proportion of 6-hydroxylated bile acid species, including alpha-muricholic acid (αMCA), beta-muricholic acid (βMCA), and the bacterial product omega-muricholic acid (ωMCA) (10, 11, 29). To determine if the CDAA diet alters the effect of ASBT inhibition on bile acid composition, the fecal bile acid profiles were determined using quantitative three-day fecal collections performed for individually-housed mice (**Figure 2**). The mass of feces excreted per day per unit body weight (g dry feces/24 h/100 g BW, mean \pm SD, $n = 9-12/\text{group}$) was similar for the CSAA vs. CDAA diet-fed mice, showed a trend toward an increase in ASBTi-treated CSAA diet-fed mice, and was significantly decreased in ASBTi-treated CDAA diet-fed mice (CSAA: 1.100 ± 0.266 vs. CSAA plus ASBTi: 1.326 ± 0.169 , $P = 0.088$; CDAA: 1.157 ± 0.230



vs. CDAA plus ASBTi: 0.908 ± 0.071 , $P = 0.02$). The fecal bile acid results are expressed as a proportion of the total amount of bile acid excreted per day per unit body weight (Figure 2A) and as the mass of individual bile acid species excreted per day per unit body weight (Figures 2B,C). For the fecal bile acid profiles, the proportion of β MCA and its bacterial product ω MCA were increased and the proportion of CA and its bacterial product DCA decreased in the CDAA vs. CSAA diet-fed mice. Following administration of the ASBTi, the fecal bile acid species

distribution became remarkably similar in the CSAA and CDAA diet-fed mice (Figure 2A). Increases were observed in excretion of the primary bile acid α MCA and secondary bile acids DCA, lithocholic acid (LCA), and hyodeoxycholic acid (HCA). The differences in fecal excretion of β MCA and ω MCA between the CSAA and CDAA-fed mice were lost after ASBTi treatment (Figures 2B,C). In addition, DCA becomes the major fecal bile acid, likely reflecting increases in bacterial 7α -dehydroxylation and possibly decreased hepatic rehydroxylation of DCA to CA



by the enzyme Cyp2a12 (30), and this was not affected by feeding a choline-deficient diet.

To assess whether dietary choline deficiency and/or ASBTi treatment affected body mass, we recorded bodyweight each week (Figure 3A). Bodyweight gain was similar for mice fed the CSAA and the CDAA diets. After 22 weeks, the increase in bodyweight was 54% and 49% ($P = 0.8$, Figure 3B) in the CSAA and CDAA diet-fed mice, respectively. The ASBTi treated groups gained less weight over the course of 22 weeks, irrespective of the diet, significantly reducing bodyweight gain by ~ 38 and 39% in the CSAA and CDAA diet-fed mice. The caloric intake was slightly higher in the ASBTi-treated CSAA group (17.8 vs. 16.3 kcal/24 h/mouse in the untreated CDAA group, $P = 0.006$) and slightly lower in the ASBTi-treated

CDAA group (14.6 vs. 16 kcal/24 h/mouse in the untreated CDAA group, $P = 0.013$, Figure 3C). Hepatomegaly due to steatosis and inflammation is a common feature of NAFLD. After 22 weeks, both absolute liver weight (2.4 vs. 3.4 g, $P = 0.001$, Figure 3D) and liver to bodyweight ratio (0.06 vs. 0.08, $P < 0.001$, Figure 3E) was increased in mice on the CDAA vs. CSAA diet. On the CSAA diet, there was a trend toward a reduced liver weight (1.9 vs. 2.4 g, $P = 0.2$, Figure 3D) and liver to bodyweight ratio (0.052 vs. 0.067, $P = 0.45$) with ASBTi treatment (Figure 3E). On the CDAA diet, liver weight (2.4 vs. 3.4, $P = 0.001$, Figure 3D) and liver to bodyweight ratio (0.059 vs. 0.084, $P = 0.001$, Figure 3E) were significantly lower with ASBTi treatment, and decreased to values similar to that in CSAA diet-fed mice.

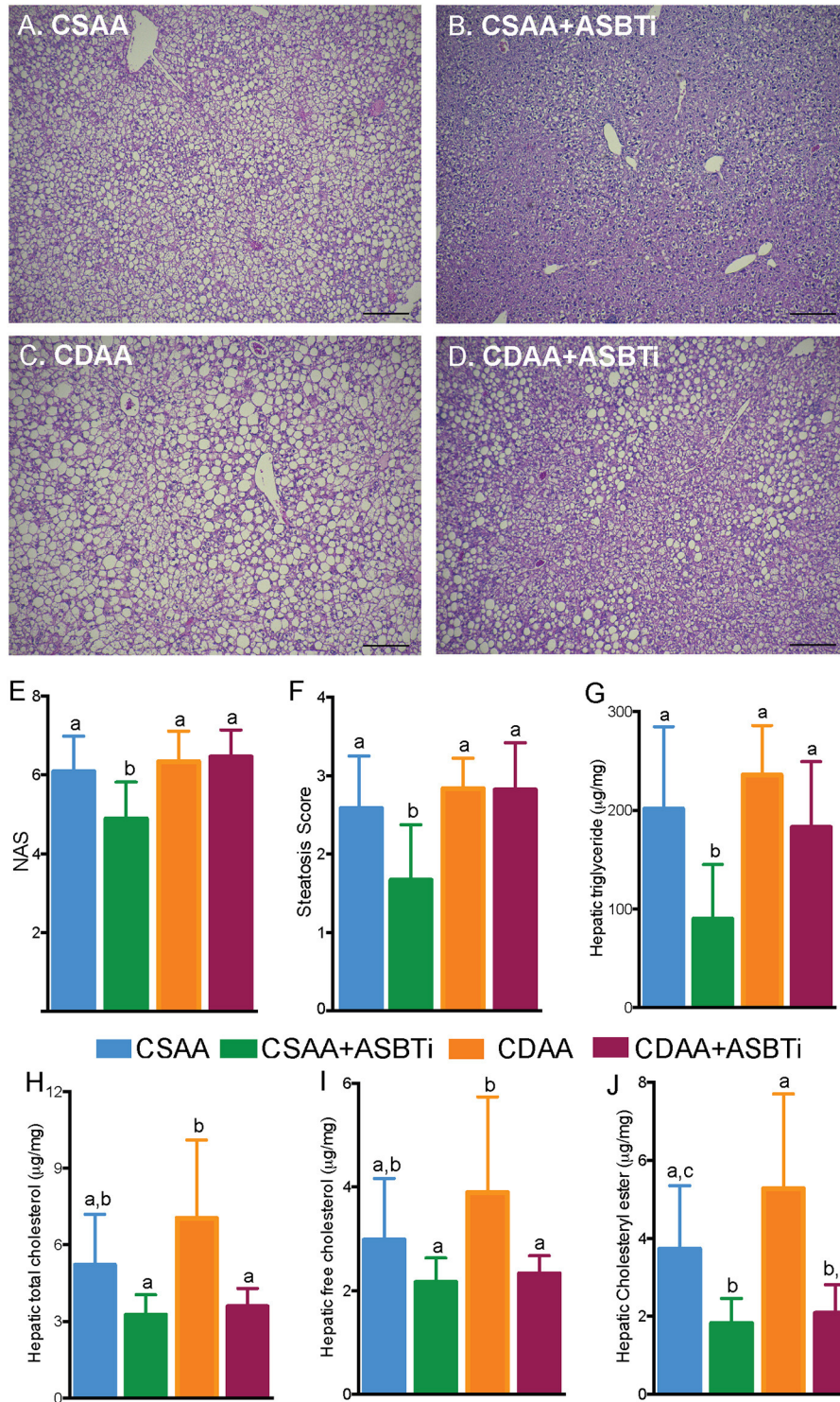
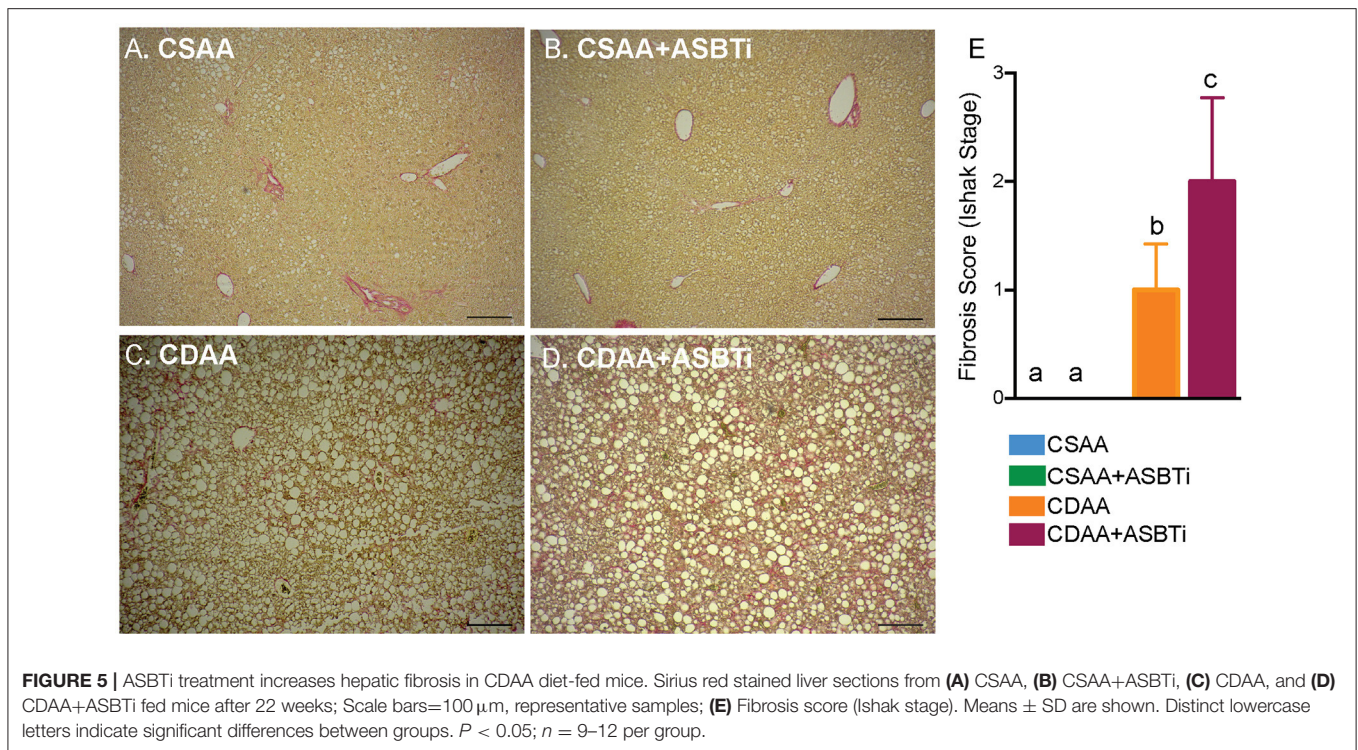


FIGURE 4 | ASBTi treatment reduces hepatic steatosis in CSAA but not CDAA diet-fed mice. Hemotoxylin and eosin stained liver sections from (A) CSAA, (B) CSAA+ASBTi, (C) CDAA, and (D) CDAA+ASBTi fed mice after 22 weeks; Scale bars = 100 µm, representative samples; (E) Non-alcoholic fatty liver disease Activity Score (NAS), (F) Steatosis score, (G) Hepatic triglyceride content, (H) Hepatic total cholesterol content, (I) Hepatic free cholesterol content, (J) Hepatic cholesteryl ester content. Means ± SD are shown. Distinct lowercase letters indicate significant differences between groups. $P < 0.05$; $n = 9-12$ per group.



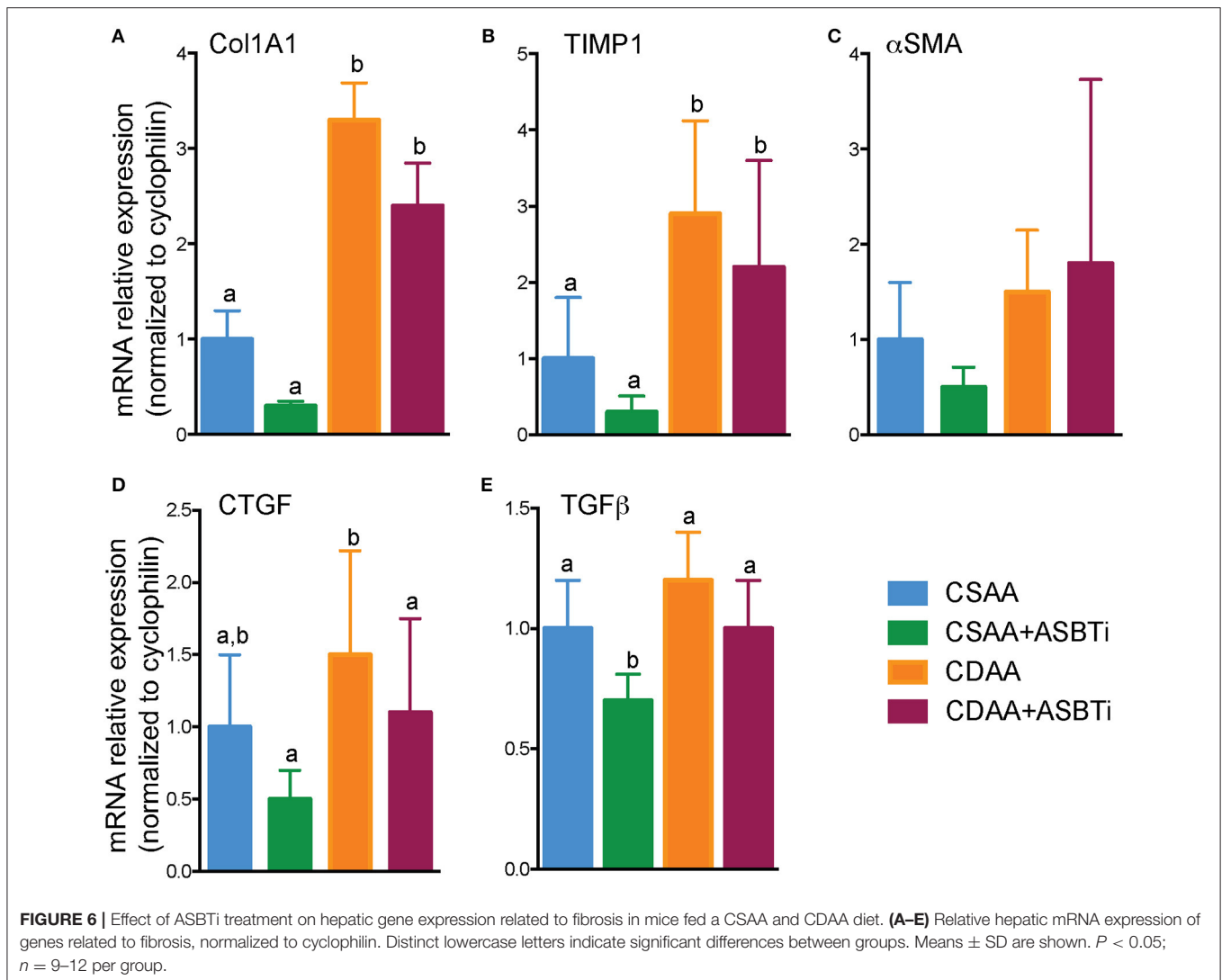
ASBT Inhibitor Treatment Reduces Hepatic Steatosis in CSAA but Not CDAA Diet-Fed Mice

To assess key features of the pathophysiology and progression of NAFLD, we examined the liver histology of the CSAA and CDAA diet-fed mice. Untreated mice fed the CSAA or CDAA diet showed clear features of NAFLD, including steatosis, lobular inflammation and hepatocyte ballooning (Figures 4A,C). Treatment with the ASBTi reduced visible lipid accumulation in mice fed the CSAA diet (Figure 4B) whereas the effects on lipid accumulation were attenuated in mice fed the CDAA diet (Figure 4D). Slides were assessed by a certified veterinary pathologist (author S.G.), who was blinded to the 4 groups, to determine NAFLD activity (NAS) and steatosis scores (Figures 4E,F). NAFLD activity (6.1 vs. 6.3, $P = 0.9$, Figure 4E) and steatosis scores (2.6 vs. 2.8, $P = 0.7$, Figure 4F) were similar for mice fed the CSAA and CDAA diets. ASBTi treatment significantly reduced the NAS and steatosis in mice fed the CSAA but not CDAA diet. To quantify hepatic lipid accumulation, we measured hepatic triglyceride and cholesterol content biochemically. In agreement with the NAS assessment, hepatic triglyceride levels were similar in mice fed the CSAA and CDAA diets (201 vs. 236 μ g/mg liver wet weight, $P = 0.6$, Figure 4G). ASBTi treatment significantly reduced hepatic triglyceride accumulation for mice fed the CSAA diet (90 vs. 201 μ g/mg liver wet weight, $P = 0.002$, Figure 4G), but the ASBTi-associated reduction in hepatic triglyceride was attenuated in mice fed the CDAA diet (183 vs. 236 μ g/mg liver wet weight, $P = 0.2$, Figure 4G). Total hepatic cholesterol content in the liver

was similar between the mice fed the low cholesterol-containing CSAA and CDAA diets (5.2 vs. 7.0 μ g/mg liver wet weight, $P = 0.1$, Figure 4H). Upon ASBTi treatment, hepatic total (3.6 vs. 7.0 μ g/mg liver wet weight, $P < 0.001$) and free cholesterol (2.3 vs. 3.9 μ g/mg liver wet weight, $P = 0.01$) levels in the CDAA diet-fed mice were reduced and a similar trend was observed for the CSAA diet (Figures 4H,I). Cholesteryl esters were significantly reduced upon ASBTi treatment for both CSAA and CDAA-fed mice (Figure 4J). Altogether, these show that ASBTi treatment reduces hepatic steatosis on the CSAA diet, in agreement with previous observations (10, 11). However, choline deficiency in the CDAA diet attenuated these effects.

ASBT Inhibitor Treatment Worsens Hepatic Fibrosis in CDAA Diet-Fed Mice

The CDAA diet has been shown to successfully induce fibrosis after feeding for 22 weeks (18, 19, 31). To visualize fibrosis on histology, collagen was stained with Sirius Red. The CSAA diet did not induce visually evident fibrosis, and treatment with the ASBTi had no visual impact on histologic Sirius Red staining (Figures 5A,B). For the CDAA diet, hepatic fibrosis was readily apparent irrespective of ASBTi treatment (Figures 5C,D). To quantify the degree of fibrosis, slides were analyzed and scored by a certified veterinary pathologist (author S.G., blinded to diet and treatment groups) using the Ishak Scoring system (24, 32). Livers of mice on the CSAA diet with or without ASBTi did not show any signs of fibrosis and received an Ishak score of 0. Mice on the CDAA diet had significantly higher fibrosis compared to the CSAA diet and received an average Ishak score of 1 (Figure 5E,



$P < 0.001$), which corresponds to a Sirius Red stained proportion of 3.0% and fibrous expansion of *some* of the portal areas with or without fibrous septa. ASBTi treatment of the CDAA diet-fed mice resulted in a significantly higher Ishak score of 2 (Figure 5E, $P = 0.02$), which corresponds to a Sirius Red stained proportion of 3.6% and fibrous expansion to *most* of the portal areas with or without short fibrous septa.

Hepatic mRNA expression of a panel of fibrosis related genes, shown previously to be upregulated by feeding the CDAA diet (31), was measured to assess whether the histological changes were reflected by the gene expression. Collagen type I alpha 1 (*Col1a1*), encoding the main component of collagen type 1 fibers, was upregulated in the CDAA diet and unaffected by ASBTi treatment (Figure 6A). Hepatic mRNA expression of tissue inhibitor of metalloproteinase-1 (*TIMP-1*), a protein involved in degradation of extracellular matrix and promoting proliferation, was similarly increased in the mice fed the CDAA diet and CDAA diet plus the ASBTi (Figure 6B). Interestingly, alpha-smooth muscle actin (α -SMA) mRNA, a marker used for

hepatic stellate cell activation (33), was unaffected by diet or treatment (Figure 6C). Connective tissue growth factor (CTGF) and transforming growth factor beta (TGF β) play important roles in fibrogenesis. Hepatic *CTGF* mRNA showed a trend toward increased expression in the CDAA vs. CSAA diet-fed mice, and was significantly decreased with ASBTi treatment in the CDAA diet-fed mice (Figure 6D). *TGF β* was similar between the CSAA and CDAA diets (Figure 6E). ASBTi treatment significantly lowered hepatic *TGF β* expression for the CSAA but not on the CDAA diet-fed mice.

As progression of liver steatosis to fibrosis generally involves inflammation, we measured hepatic gene expression of several important inflammatory genes. Expression of the proinflammatory genes tumor necrosis factor α (*TNF α*), inducible nitric oxide synthase (*iNOS*), and monocyte chemoattractant protein 1 (*MCP1*) were upregulated in the CDAA vs. CSAA diet-fed mice and unaffected by ASBTi treatment (Figures 7A–C). Hepatic cell damage and increases in inflammation are often paired with oxidative stress. Therefore,

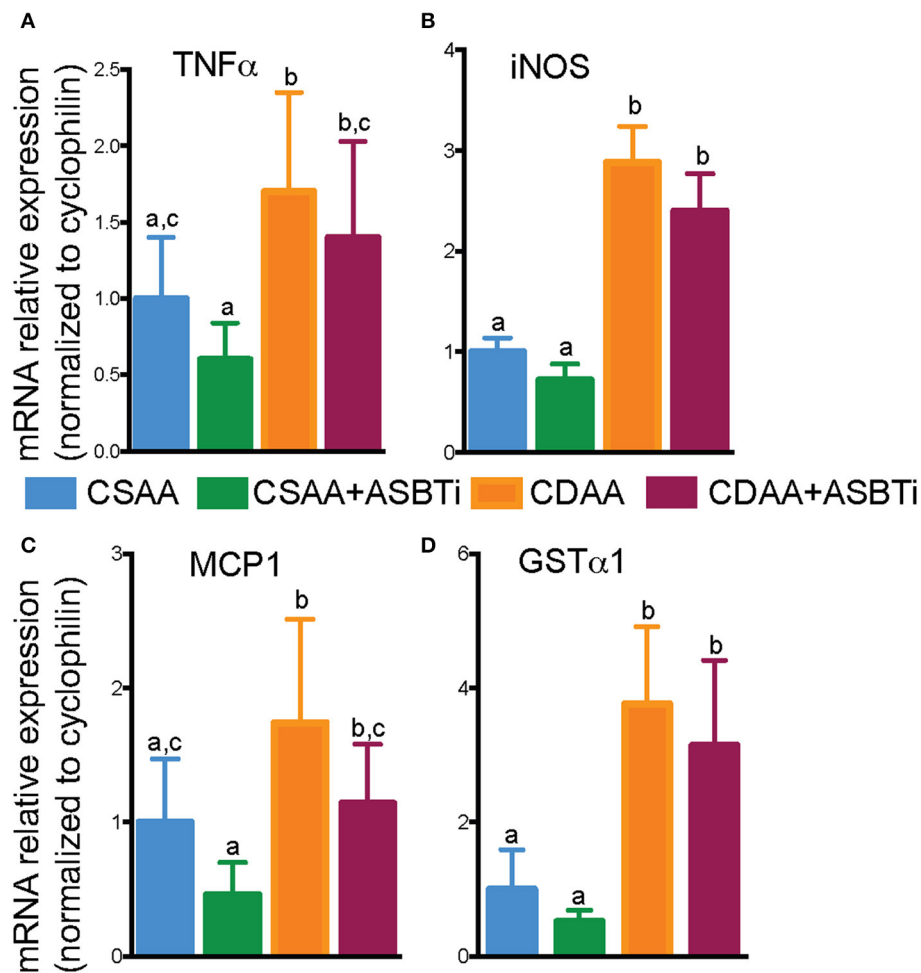


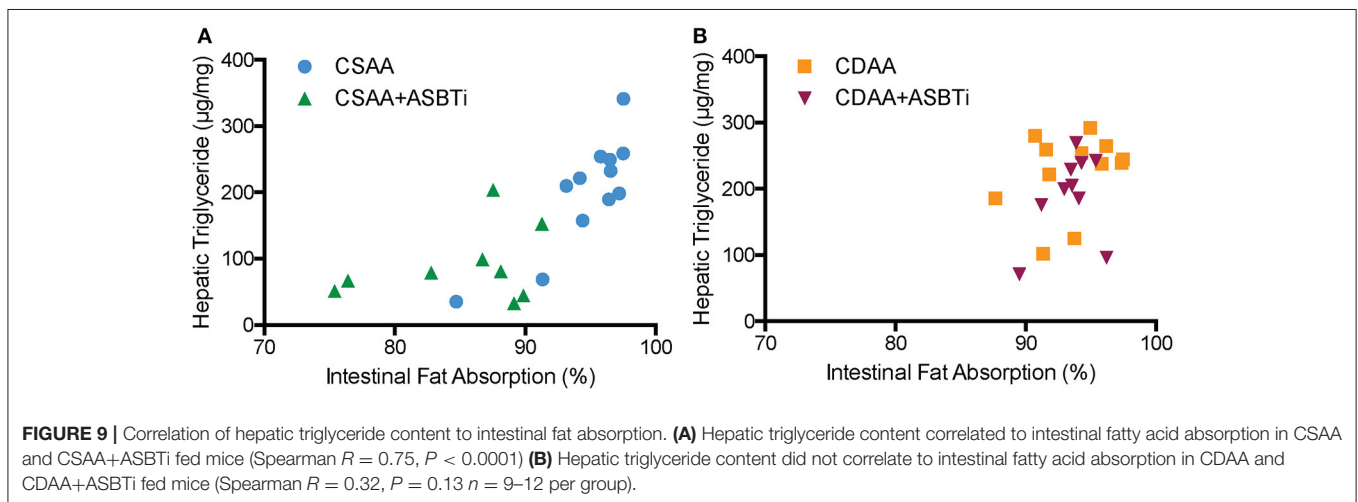
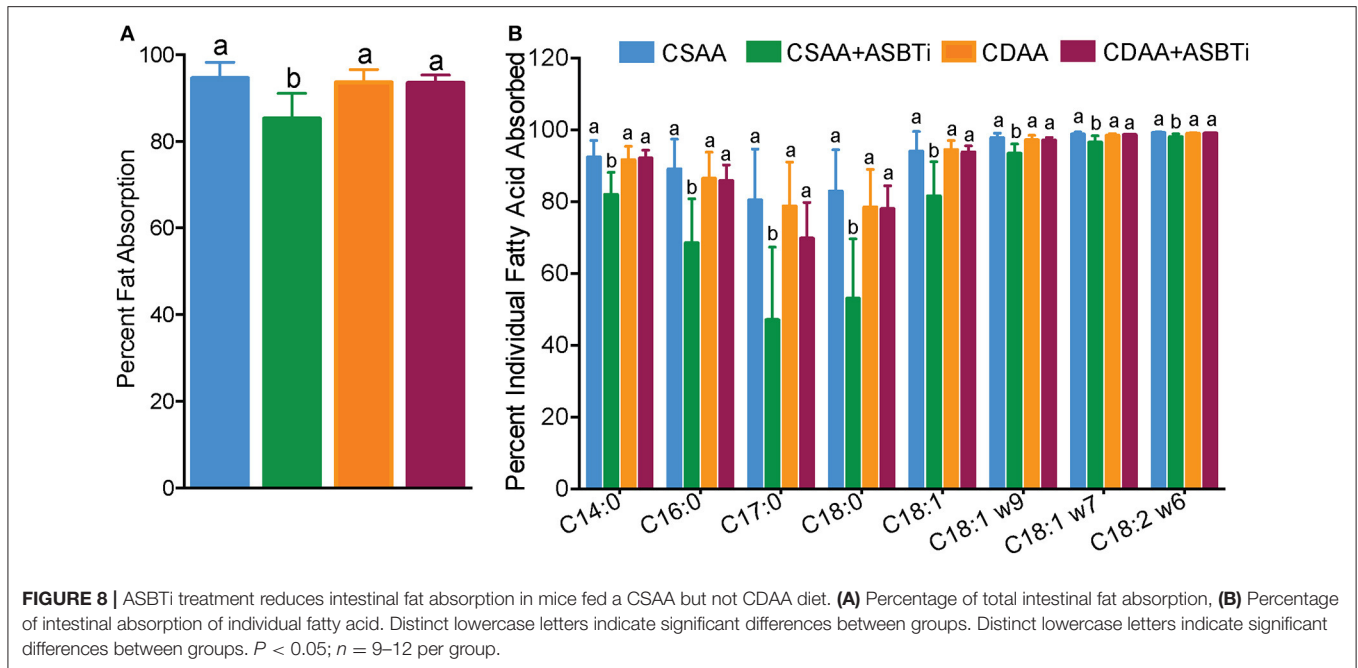
FIGURE 7 | Effect of ASBTi treatment on hepatic gene expression related to inflammation in mice fed a CSAA and CDAA diet. **(A–D)** Relative hepatic mRNA expression of genes related to inflammation, normalized to cyclophilin. Means \pm SD are shown. Distinct lowercase letters indicate significant differences between groups. $P < 0.05$; $n = 9$ – 12 per group.

we measured glutathione S-transferase A1 (*GST α 1*) expression, the gene encoding a key enzyme in the anti-oxidative glutathione pathway. *GST α 1* expression was increased upon feeding the CDAA vs. CSAA diet but unaffected by ASBTi treatment (Figure 7D). Altogether, these data suggest that the ASBTi treatment was not able to prevent inflammation, oxidative stress or fibrosis in this dietary choline deficiency mouse model of NAFLD/NASH.

ASBT Inhibitor Treatment Reduces Intestinal Fat Absorption in CSAA but Not CDAA Diet-Fed Mice

We previously reported that genetic ASBT knockout in mice reduces intestinal fat and cholesterol absorption (29, 34, 35). In order to determine if the ASBTi treatment had similar effects in the CSAA and CDAA diet-fed mice, we measured fat absorption using the sucrose polybehenate method (20). For mice on the

CSAA diet, ASBTi treatment reduced total fatty acid absorption by almost 10% (85.3 vs. 94.6%, $P < 0.001$, Figure 8A). The ASBTi treatment-associated decrease in fat absorption in the CSAA diet-fed mice was greater for the saturated fatty acids myristic acid (C14:0), palmitic acid (C16:0), margaric acid (C17:0), and stearic acid (C18:0) followed by the *trans* saturated fatty acid, elaidic acid (C18:1 ω 9) (Figure 8B). For the group of saturated fatty acids, the ASBTi treatment effect on absorption increased with fatty acid acyl chain length, which corresponds to greater hydrophobicity and correlates with increased bile acid requirement for efficient micellar solubilization (36). The ASBTi treatment-associated decreases in fat absorption in the CSAA diet-fed mice for the mono- and polyunsaturated fatty acids oleic acid (C18:1 ω 9), vaccenic acid (C18:1 ω 7), and linoleic acid (C18:2 ω 6) were also statistically significant but the absolute differences were smaller (Figure 8B). We found no difference in total fat absorption between the mice fed the CSAA and the CDAA diets (94.6 vs. 93.6%, $P = 0.9$, Figure 8A). However, in contrast to mice



fed the CSAA diet, absorption of neither total fat (93.5 vs. 93.6%, $P = 1.0$, **Figure 8A**) or the individual fatty acids were affected by ASBTi treatment of CDAA diet-fed mice. Correlation analysis showed that the hepatic triglyceride content is highly correlated to intestinal fatty acid absorption in mice fed the CSAA (Spearman $R = 0.75$, $P < 0.001$, **Figure 9A**) but not CDAA diet (Spearman $R = 0.32$, $P = 0.9$, **Figure 9B**).

Although we did not directly assess cholesterol absorption in the current study, we measured fecal excretion of neutral sterols, cholesterol and its fecal metabolites. Fecal neutral excretion ($\mu\text{mol}/24 \text{ h}/100 \text{ g BW}$, mean \pm SD, $n = 9-12$ per group) was significantly higher in CSAA mice treated with an ASBTi compared to CSAA control mice (CSAA plus ASBTi: 12.0 ± 4.8 vs. CSAA: 7.5 ± 3.3 , $P = 0.02$). On the CDAA diet, fecal neutral sterol excretion was comparable to the CSAA diet (CDAA: 9.7

± 3.2 vs. CSAA: 7.5 ± 3.3 , $P = 0.4$). However, in contrast to the CSAA diet, ASBTi treatment did not significantly increase fecal neutral sterol excretion in mice fed the CDAA diet (CDAA plus ASBTi: 8.0 ± 1.2 vs. 9.7 ± 3.2 , $P = 0.6$). Previous studies have suggested that feeding a choline-deficient diet can promote triglyceride accumulation in enterocytes as a result of impaired chylomicron secretion (37, 38). In this study, there was a trend toward increased jejunal tissue triglyceride in CDAA vs. CSAA diet-fed mice, but the differences were not statistically significant ($P > 0.05$) and there was no effect of ASBTi treatment on the jejunal tissue triglyceride (μg per g tissue, mean \pm SD, $n = 9-12$ per group; CSAA: 23.2 ± 10.5 ; CSAA plus ASBTi: 22.8 ± 9.2 ; CDAA: 29.8 ± 9.2 ; CDAA plus ASBTi: 33.01 ± 10.7). The jejunal tissue total cholesterol content (μg per g tissue, mean \pm SD, $n = 9-12$ per group) was also not different ($P > 0.05$) between

the different groups (CSAA: 2.5 ± 0.2 ; CSAA plus ASBTi: 2.31 ± 0.23 ; CDAA: 2.27 ± 0.28 ; CDAA plus ASBTi: 2.22 ± 0.39).

DISCUSSION

In the current study, we showed that treatment with an ASBTi did not prevent development of hepatic fibrosis in a CDAA diet-fed mouse model. Additionally, under dietary choline-deficient conditions, previously reported effects of ASBT inhibition on fat and cholesterol absorption were nullified, possibly contributing to the phenotype. Dietary interventions in mouse models to reproducibly induce NASH and fibrosis are limited. The CDAA diet was used in the current study because, contrary to the MCD diet, the CDAA diet was shown to successfully induce hepatic fibrosis without significantly lowering bodyweight and plasma glucose levels (18, 19). Approximately 95% of the choline in animal tissues is present as phosphatidylcholine (PC), a major component of membranes (39). The primary mechanism believed to be involved in the effects of choline deficiency on hepatic steatosis is impairment of VLDL secretion due to insufficient PC (15). Interestingly, bile acid sequestrants act similar to ASBT inhibition by interrupting the enterohepatic circulation of bile acids, and have been shown to increase plasma VLDL and triglyceride levels (40–42). Therefore, one of the mechanisms contributing to the anti-steatotic actions of ASBTi treatment may be increasing hepatic VLDL secretion and triglyceride export from the liver, which is attenuated under choline-deficient conditions.

In addition to affecting VLDL secretion, choline deficiency alters mitochondrial function (43), fatty acid beta-oxidation (44), and changes epigenetic marking (45). Choline deficiency also alters the intestinal microbiota, which may be involved in the development of NAFLD (46). Treatment with the ASBTi induces similar changes in the fecal bile acid profile for the CSAA and CDAA diet-fed mice, such that the fecal bile acid composition including the microbiota-derived secondary bile acids is almost identical for the two ASBTi-treated groups. Changes in the gut microbiota composition associated with feeding the choline-deficient amino acid-defined diet have been reported previously (47). However, the almost identical fecal secondary bile acid profiles suggests that at least this aspect (bile acid biotransformation) of the gut microbiome actions does not appear to account for the differential response of the CSAA and CDAA diet-fed mice to the ASBTi. It was previously shown that treatment of high fat diet-fed mice with the ASBTi for 16 weeks shifted the hepatic bile acid composition shifted toward a more hydrophobic and thus potentially cytotoxic profile (10). *In vitro* studies have shown that PC protects hepatocytes from bile acid-induced cytotoxicity (48, 49). Although not injurious when hepatic PC synthesis is intact, the ASBTi-induced shift to a more hydrophobic bile acid pool may be injurious under PC-deficient conditions. The absence of beneficial effects in the CDAA model has been noted for other therapeutic interventions such as FXR agonism with obeticholic acid (50). Moreover, feeding a choline-deficient, iron-supplemented L-amino acid-defined diet to rats has been shown to induce a persistent fibrosis, potentially secondary to increased oxidative stress (51). This later observation is particularly important since it has recently been

shown that interrupting the enterohepatic circulation of bile acids in mice decreases hepatic glutathione levels and impairs glutathione regenerating capacity (52). This is due in part to increased expression of cysteine dioxygenase type 1, in order to shunt cysteine toward taurine biosynthesis to meet the increased demand for synthesis of taurine-conjugated bile acids. A decrease in hepatic cysteine and glutathione levels combined with choline deficiency may underlie the increase in fibrosis observed in the ASBTi-treated CDAA diet-fed mice. However, these results should be interpreted with caution in regard to human NAFLD/NASH pathophysiology, as this rarely involves choline deficiency (53) and humans preferentially use glycine vs. taurine for bile acid conjugation (54). Future studies using different models are needed for understand the potential impact of ASBTi treatment on NASH and fibrosis. Fortunately, several recently developed murine NAFLD models have shown promising results in mimicking human NAFLD/NASH pathophysiology (55, 56).

Anti-steatotic effects of ASBT pharmacological inhibition have been a consistent finding in high fat diet-fed mouse models, including the CSAA diet-fed mice in this study (10, 11), and we previously observed inhibitory effects of ASBT genetic inactivation on intestinal cholesterol and fat absorption (29, 34, 35). In our current study, ASBTi treatment lowered fatty acid absorption and intestinal fat absorption positively correlated with hepatic triglyceride levels in the CSAA diet-fed mice. By contrast in the choline-deficient CDAA diet-fed mice, ASBTi-treatment had no effect on intestinal fat absorption and the hepatic anti-steatotic effects were attenuated. The mechanisms underlying our observations in the CDAA-fed mice remain unclear. Intestinal intraluminal PC concentrations contribute to mixed micelle formation, lipid transport across the unstirred water layer, and subsequent lipid translocation to the brush border membrane (57). In rats, dietary choline deficiency was shown to decrease chylomicron secretion and alter intestinal cell morphology and physiology, resulting in impairments of dietary fat absorption (37, 38). One could speculate that intestinal adaptations present in the choline-deficient CDAA diet-fed mice to compensate for decreased biliary PC affect lipolytic and post-lipolytic events related to intestinal lipid absorption. The absence of a protective effect on hepatic steatosis for interventions that act via reduced intestinal fat absorption has been observed previously in dietary choline-deficient models. For example, intestine-specific knockout of the zinc finger transcription factor GATA4 reduces intestinal lipid absorption and was protective against hepatic steatosis induced by feeding a high fat but not MCD diet (58).

In conclusion, this study showed that ASBTi treatment did not affect intestinal fat absorption and was not protective against hepatic fibrosis in a choline-deficient mouse model of NASH. Nevertheless, these findings add to our understanding of the uses and limitations of dietary choline-deficient mouse and the potential mechanisms by which interrupting the enterohepatic circulation of bile acids may impact development of NAFLD and NASH. Indirectly modulating intestinal fat absorption via ASBTi treatment is an interesting potential therapeutic target. Future studies using different models for NASH are warranted to further understand the relationship between bile acids and the progression of hepatic steatosis to NASH and fibrosis.

DATA AVAILABILITY STATEMENT

The datasets generated for this study are available on request to the corresponding author.

ETHICS STATEMENT

The animal study was reviewed and approved by Emory University Institutional Animal Care and Use Committee.

AUTHOR CONTRIBUTIONS

AR, IP, and SG performed the experiments and collected and analyzed the data. AR managed the study. AR, SK, and PD designed the study and conceived the experiments. PD, IP, AR, and SK wrote the paper.

FUNDING

This study was supported by the NIH (DK047987 to PD and DK56239 to SK). PD and SK are also supported by the Center

for Transplantation and Immune-mediated Disorders and the Children's Healthcare of Atlanta.

ACKNOWLEDGMENTS

We thank Lumena/Shire for the research gift of the ASBTi (SC-435), Dr. D. Shayakhmetov (Emory University School of Medicine) for assistance with the microscopy, Matthew Davis (Lipoprotein Analysis Laboratory at Wake Forest University School of Medicine) for fatty acid analysis, the Children's Healthcare of Atlanta pathology Services for processing tissues for histology, and the Yerkes Nonhuman Primate Molecular Pathology Core for assistance with Sirius Red staining. We also thank Kim Pachura for assistance with the mouse necropsies. Portions of this work were presented at the Annual Meeting of the American Gastroenterology Association in San Diego, CA, 18–21 May 2019 and have appeared in abstract form *Gastroenterology*. 156 (6), Supplement 1, S-1296 (Su1556). Portions of this work are also included in an author's doctoral thesis in accordance with the author's University policy (59).

REFERENCES

- Estes C, Anstee QM, Arias-Loste MT, Bantel H, Bellentani S, Caballeria J, et al. Modeling NAFLD disease burden in China, France, Germany, Italy, Japan, Spain, United Kingdom, and United States for the period 2016–2030. *J Hepatol*. (2018) 69:896–904. doi: 10.1016/j.jhep.2018.05.036
- Younossi Z, Anstee QM, Marietti M, Hardy T, Henry L, Eslam M, et al. Global burden of NAFLD and NASH: trends, predictions, risk factors and prevention. *Nat Rev Gastroenterol Hepatol*. (2018) 15:11–20. doi: 10.1038/nrgastro.2017.109
- Byrne CD, Targher G. NAFLD: a multisystem disease. *J Hepatol*. (2015) 62:S47–64. doi: 10.1016/j.jhep.2014.12.012
- Friedman SL, Neuschwander-Tetri BA, Rinella M, Sanyal AJ. Mechanisms of NAFLD development and therapeutic strategies. *Nat Med*. (2018) 24:908–22. doi: 10.1038/s41591-018-0104-9
- Chavez-Talavera O, Tailleux A, Lefebvre P, Staels B. Bile acid control of metabolism and inflammation in obesity, type 2 diabetes, dyslipidemia, and nonalcoholic fatty liver disease. *Gastroenterology*. (2017) 152:1679–94.e3. doi: 10.1053/j.gastro.2017.01.055
- Ridlon JM, Harris SC, Bhowmik S, Kang DJ, Hylemon PB. Consequences of bile salt biotransformations by intestinal bacteria. *Gut Microbes*. (2016) 7:22–39. doi: 10.1080/19490976.2015.1127483
- Wahlstrom A, Sayin SI, Marschall HU, Backhed F. Intestinal crosstalk between bile acids and microbiota and its impact on host metabolism. *Cell Metab*. (2016) 24:41–50. doi: 10.1016/j.cmet.2016.05.005
- Mudaliar S, Henry RR, Sanyal AJ, Morrow L, Marschall HU, Kipnes M, et al. Efficacy and safety of the farnesoid X receptor agonist obeticholic acid in patients with type 2 diabetes and nonalcoholic fatty liver disease. *Gastroenterology*. (2013) 145:574–82.e1. doi: 10.1053/j.gastro.2013.05.042
- Neuschwander-Tetri BA, Loomba R, Sanyal AJ, Lavine JE, Van Natta ML, Abdelmalek MF, et al. Farnesoid X nuclear receptor ligand obeticholic acid for non-cirrhotic, non-alcoholic steatohepatitis (FLINT): a multicentre, randomised, placebo-controlled trial. *Lancet*. (2015) 385:956–65. doi: 10.1016/S0140-6736(14)61933-4
- Rao A, Kosters A, Mells JE, Zhang W, Setchell KD, Amanso AM, et al. Inhibition of ileal bile acid uptake protects against nonalcoholic fatty liver disease in high-fat diet-fed mice. *Sci Transl Med*. (2016) 8:357ra122. doi: 10.1126/scitranslmed.aaf4823
- Salic K, Kleemann R, Wilkins-Port C, McNulty J, Verschuren L, Palmer M. Apical sodium-dependent bile acid transporter inhibition with volixibat improves metabolic aspects and components of non-alcoholic steatohepatitis in Ldlr-/-Leiden mice. *PLoS ONE*. (2019) 14:e0218459. doi: 10.1371/journal.pone.0218459
- Lau JK, Zhang X, Yu J. Animal models of non-alcoholic fatty liver disease: current perspectives and recent advances. *J Pathol*. (2017) 241:36–44. doi: 10.1002/path.4829
- Denk H, Abuja PM, Zatloukal K. Animal models of NAFLD from the pathologist's point of view. *Biochim Biophys Acta Mol Basis Dis*. (2019) 1865:929–42. doi: 10.1016/j.bbdis.2018.04.024
- Jahn D, Kircher S, Hermanns HM, Geier A. Animal models of NAFLD from a hepatologist's point of view. *Biochim Biophys Acta Mol Basis Dis*. (2019) 1865:943–53. doi: 10.1016/j.bbdis.2018.06.023
- Corbin KD, Zeisel SH. Choline metabolism provides novel insights into nonalcoholic fatty liver disease and its progression. *Curr Opin Gastroenterol*. (2012) 28:159–65. doi: 10.1097/MOG.0b013e32834e7b4b
- Rinella ME, Green RM. The methionine-choline deficient dietary model of steatohepatitis does not exhibit insulin resistance. *J Hepatol*. (2004) 40:47–51. doi: 10.1016/j.jhep.2003.09.020
- Machado MV, Michelotti GA, Xie G, Almeida Pereira T, Boursier J, Bohnic B, et al. Mouse models of diet-induced nonalcoholic steatohepatitis reproduce the heterogeneity of the human disease. *PLoS ONE*. (2015) 10:e0127991. doi: 10.1371/journal.pone.0127991
- Miura K, Kodama Y, Inokuchi S, Schnabl B, Aoyama T, Ohnishi H, et al. Toll-like receptor 9 promotes steatohepatitis by induction of interleukin-1beta in mice. *Gastroenterology*. (2010). 139:323–34.e7. doi: 10.1053/j.gastro.2010.03.052
- Pizarro M, Solis N, Quintero P, Barrera F, Cabrera D, Rojas-de Santiago P, et al. Beneficial effects of mineralocorticoid receptor blockade in experimental non-alcoholic steatohepatitis. *Liver Int*. (2015) 35:2129–38. doi: 10.1111/liv.12794
- Jandacek RJ, Heubi JE, Tso P. A novel, noninvasive method for the measurement of intestinal fat absorption. *Gastroenterology*. (2004) 127:139–44. doi: 10.1053/j.gastro.2004.04.007
- Simon T, Cook VR, Rao A, Weinberg RB. Impact of murine intestinal apolipoprotein A-IV expression on regional lipid absorption, gene expression, and growth. *J Lipid Res*. (2011) 52:1984–94. doi: 10.1194/jlr.M017418
- Sun H, Hu Y, Gu Z, Wilson MD, Chen YQ, Rudel LL, et al. Endogenous synthesis of n-3 polyunsaturated fatty acids in Fat-1 mice is associated with increased mammary gland and liver syndecan-1. *PLoS ONE*. (2011) 6:e20502. doi: 10.1371/journal.pone.0020502
- Kleiner DE, Brunt EM, Van Natta M, Behling C, Contos MJ, Cummings OW, et al. Design and validation of a histological scoring system for nonalcoholic

- fatty liver disease. *Hepatology*. (2005) 41:1313–21. doi: 10.1002/hep.20701
24. Ishak K, Baptista A, Bianchi L, Callea F, De Groote J, Gudat F, et al. Histological grading and staging of chronic hepatitis. *J Hepatol*. (1995) 22:696–9. doi: 10.1016/0168-8278(95)80226-6
 25. Folch J, Lees M, Sloane Stanley GH. A simple method for the isolation and purification of total lipides from animal tissues. *J Biol Chem*. (1957) 226:497–509.
 26. Rao A, Haywood J, Craddock AL, Belinsky MG, Kruh GD, Dawson PA. The organic solute transporter alpha-beta, Ostalpha-Ostbeta, is essential for intestinal bile acid transport and homeostasis. *Proc Natl Acad Sci USA*. (2008) 105:3891–6. doi: 10.1073/pnas.0712328105
 27. van Meer H, Boehm G, Stellaard F, Vriesema A, Knol J, Havinga R, et al. Prebiotic oligosaccharides and the enterohepatic circulation of bile salts in rats. *Am J Physiol Gastrointest Liver Physiol*. (2008) 294:G540–7. doi: 10.1152/ajpgi.00396.2007
 28. Gamble W, Vaughan M, Kruth HS, Avigan J. Procedure for determination of free and total cholesterol in micro- or nanogram amounts suitable for studies with cultured cells. *J Lipid Res*. (1978) 19:1068–70.
 29. van de Peppel IP, Bertolini A, van Dijk TH, Groen AK, Jonker JW, Verkade HJ. Efficient reabsorption of transintestinally excreted cholesterol is a strong determinant for cholesterol disposal in mice. *J Lipid Res*. (2019) 60:1562–72. doi: 10.1194/jlr.M094607
 30. Honda A, Miyazaki T, Iwamoto J, Hirayama T, Morishita Y, Monma T, et al. Regulation of bile acid metabolism in mouse models with hydrophobic bile acid composition. *J Lipid Res*. (2020) 61:54–69. doi: 10.1194/jlr.RA119000395
 31. Cabrera D, Wree A, Povero D, Solis N, Hernandez A, Pizarro M, et al. Andrographolide ameliorates inflammation and fibrogenesis and attenuates inflammatory activation in experimental non-alcoholic steatohepatitis. *Sci Rep*. (2017) 7:3491. doi: 10.1038/s41598-017-03675-z
 32. Standish RA, Cholongitas E, Dhillon A, Burroughs AK, Dhillon AP. An appraisal of the histopathological assessment of liver fibrosis. *Gut*. (2006) 55:569–78. doi: 10.1136/gut.2005.084475
 33. Carpino G, Morini S, Ginanni Corradini S, Franchitto A, Merli M, Siciliano M, et al. Alpha-SMA expression in hepatic stellate cells and quantitative analysis of hepatic fibrosis in cirrhosis and in recurrent chronic hepatitis after liver transplantation. *Dig Liver Dis*. (2005) 37:349–56. doi: 10.1016/j.dld.2004.11.009
 34. Dawson PA, Haywood J, Craddock AL, Wilson M, Tietjen M, Kluckman K, et al. Targeted deletion of the ileal bile acid transporter eliminates enterohepatic cycling of bile acids in mice. *J Biol Chem*. (2003) 278:33920–7. doi: 10.1074/jbc.M306370200
 35. Dawson PA. Impact of inhibiting ileal apical versus basolateral bile acid transport on cholesterol metabolism and atherosclerosis in mice. *Dig Dis*. (2015) 33:382–7. doi: 10.1159/000371691
 36. McKimmie RL, Easter L, Weinberg RB. Acyl chain length, saturation, and hydrophobicity modulate the efficiency of dietary fatty acid absorption in adult humans. *Am J Physiol Gastrointest Liver Physiol*. (2013) 305:G620–627. doi: 10.1152/ajpgi.00258.2013
 37. Takahashi Y, Mizunuma T, Kishino Y. Effects of choline deficiency and phosphatidylcholine on fat absorption in rats. *J Nutr Sci Vitaminol*. (1982) 28:139–47. doi: 10.3177/jnsv.28.139
 38. da Silva RP, Kelly KB, Lewis ED, Leonard KA, Goruk S, Curtis JM, et al. Choline deficiency impairs intestinal lipid metabolism in the lactating rat. *J Nutr Biochem*. (2015) 26:1077–83. doi: 10.1016/j.jnutbio.2015.04.015
 39. Li Z, Vance DE. Phosphatidylcholine and choline homeostasis. *J Lipid Res*. (2008) 49:1187–94. doi: 10.1194/jlr.R700019-JLR200
 40. Beil U, Crouse JR, Einarsson K, Grundy SM. Effects of interruption of the enterohepatic circulation of bile acids on the transport of very low density-lipoprotein triglycerides. *Metabolism*. (1982) 31:438–44. doi: 10.1016/0026-0495(82)90231-1
 41. Watanabe M, Houten SM, Wang L, Moschetta A, Mangelsdorf DJ, Heyman RA, et al. Bile acids lower triglyceride levels via a pathway involving FXR, SHP, and SREBP-1c. *J Clin Invest*. (2004) 113:1408–18. doi: 10.1172/JCI21025
 42. Mazidi M, Rezaei P, Karimi E, Kengne AP. The effects of bile acid sequestrants on lipid profile and blood glucose concentrations: a systematic review and meta-analysis of randomized controlled trials. *Int J Cardiol*. (2017) 227:850–7. doi: 10.1016/j.ijcard.2016.10.011
 43. Teodoro JS, Rolo AP, Duarte FV, Simoes AM, Palmeira CM. Differential alterations in mitochondrial function induced by a choline-deficient diet: understanding fatty liver disease progression. *Mitochondrion*. (2008) 8:367–76. doi: 10.1016/j.mito.2008.07.008
 44. Serviddio G, Giudetti AM, Bellanti F, Priore P, Rollo T, Tamborra R, et al. Oxidation of hepatic carnitine palmitoyl transferase-I (CPT-I) impairs fatty acid beta-oxidation in rats fed a methionine-choline deficient diet. *PLoS ONE*. (2011) 6:e24084. doi: 10.1371/journal.pone.0024084
 45. Mehedin MG, Niculescu MD, Craciunescu CN, Zeisel SH. Choline deficiency alters global histone methylation and epigenetic marking at the Re1 site of the calbindin 1 gene. *FASEB J*. (2010) 24:184–95. doi: 10.1096/fj.09-140145
 46. Tremaroli V, Backhed F. Functional interactions between the gut microbiota and host metabolism. *Nature*. (2012) 489:242–9. doi: 10.1038/nature11552
 47. Ishioka M, Miura K, Minami S, Shimura Y, Ohnishi H. Altered gut microbiota composition and immune response in experimental steatohepatitis mouse models. *Dig Dis Sci*. (2017) 62:396–406. doi: 10.1007/s10620-016-4393-x
 48. Ikeda Y, Morita SY, Terada T. Cholesterol attenuates cytoprotective effects of phosphatidylcholine against bile salts. *Sci Rep*. (2017) 7:306. doi: 10.1038/s41598-017-00476-2
 49. Morita SY, Ikeda Y, Tsuji T, Terada T. Molecular mechanisms for protection of hepatocytes against bile salt cytotoxicity. *Chem Pharm Bull*. (2019) 67:333–40. doi: 10.1248/cpb.c18-01029
 50. Tolbol KS, Stierstorfer B, Rippmann JF, Veidal SS, Rigbolt KTG, Schonberger T, et al. Disease progression and pharmacological intervention in a nutrient-deficient rat model of nonalcoholic steatohepatitis. *Dig Dis Sci*. (2019) 64:1238–56. doi: 10.1007/s10620-018-5395-7
 51. Takeuchi-Yorimoto A, Noto T, Yamada A, Miyamae Y, Oishi Y, Matsumoto M. Persistent fibrosis in the liver of choline-deficient and iron-supplemented L-amino acid-defined diet-induced nonalcoholic steatohepatitis rat due to continuing oxidative stress after choline supplementation. *Toxicol Appl Pharmacol*. (2013) 268:264–77. doi: 10.1016/j.taap.2013.01.027
 52. Wang Y, Li J, Matye D, Zhang Y, Dennis K, Ding WX, et al. Bile acids regulate cysteine catabolism and glutathione regeneration to modulate hepatic sensitivity to oxidative injury. *JCI Insight*. (2018) 3:e99676. doi: 10.1172/jci.insight.99676
 53. Guerrero AL, Colvin RM, Schwartz AK, Molleston JP, Murray KF, Diehl A, et al. Choline intake in a large cohort of patients with nonalcoholic fatty liver disease. *Am J Clin Nutr*. (2012) 95:892–900. doi: 10.3945/ajcn.111.020156
 54. Li J, Dawson PA. Animal models to study bile acid metabolism. *Biochim Biophys Acta Mol Basis Dis*. (2019) 1865:895–911. doi: 10.1016/j.bbadis.2018.05.011
 55. Hui ST, Kurt Z, Tuominen I, Norheim F, Davis RC, Pan C, et al. The genetic architecture of diet-induced hepatic fibrosis in mice. *Hepatology*. (2018) 68:2182–96. doi: 10.1002/hep.30113
 56. Tsuchida T, Lee YA, Fujiwara N, Ybanez M, Allen B, Martins S, et al. A simple diet- and chemical-induced murine NASH model with rapid progression of steatohepatitis, fibrosis and liver cancer. *J Hepatol*. (2018) 69:385–95. doi: 10.1016/j.jhep.2018.03.011
 57. Noh SK, Koo SI. Enteral infusion of phosphatidylcholine increases the lymphatic absorption of fat, but lowers alpha-tocopherol absorption in rats fed a low zinc diet. *J Nutr Biochem*. (2001) 12:330–7. doi: 10.1016/S0955-2863(01)00145-0
 58. Patankar JV, Obrowsky S, Doddapattar P, Hoefler G, Battle M, Levak-Frank S, et al. Intestinal GATA4 deficiency protects from diet-induced hepatic steatosis. *J Hepatol*. (2012) 57:1061–8. doi: 10.1016/j.jhep.2012.06.028
 59. van de Peppel IP. *Intestinal Bile Acid Reabsorption in Health and Disease*. Rijksuniversiteit Groningen (2019).
- Conflict of Interest:** The authors declare that the research was conducted in the absence of any commercial or financial relationships that could be construed as a potential conflict of interest.
- Copyright © 2020 Rao, Peppel, Gumber, Karpen and Dawson. This is an open-access article distributed under the terms of the Creative Commons Attribution License (CC BY). The use, distribution or reproduction in other forums is permitted, provided the original author(s) and the copyright owner(s) are credited and that the original publication in this journal is cited, in accordance with accepted academic practice. No use, distribution or reproduction is permitted which does not comply with these terms.